Evaluation of convective parameterization schemes in simulation of tropical cyclones by Climate Forecast System model: Version 2

Radhika D Kanase, Medha S Deshpande, R P M Krishna
and Parthasarathi Mukhopadhyay*

Indian Institute of Tropical Meteorology, Ministry of Earth Sciences, Pashan, Pune 411 008, India.
Corresponding author. e-mail: mpartha@tropmet.res.in

Recently, a high resolution atmospheric general circulation model, i.e., Global Forecast System has been operationalized for 10 days weather forecast over Indian region. However, for extreme weather systems such as cyclones, different physical processes and their interactions with atmosphere and ocean play an important role in cyclone intensity, track, etc. Keeping this in view, Coupled Forecast System model version 2 has been used to evaluate the simulation for three severe cyclones (Phailin, Viyaru and Lehar) of 2013. In the present study, along with already existing mass-flux cumulus parameterization, i.e., Simplified Arakawa–Schubert (SAS) and revised SAS (RSAS) parameterization schemes, an additional convective adjustment scheme, i.e., Betts–Miller–Janjic (BMJ) is implemented and its performance is evaluated for the Indian Ocean cyclones. The experiments are conducted with three cumulus schemes at three different resolutions (T126, T382, and T574). Both SAS and RSAS overestimate convective rain, whereas BMJ scheme produces convective rain comparable with the observation due to the fact that BMJ produces deeper convection and does not trigger the convection too often. BMJ sustains the instability and deep convection longer thereby impacting the cyclone intensity and heavy rainfall associated with it. It is also noted that BMJ is efficient in producing rain than the SAS and RSAS. From the analyses of OLR and rain rate, BMJ is found to simulate a much realistic relation of cloud and precipitation. The paper argues that compared to available SAS and RSAS, BMJ scheme realistically produces heavy precipitation associated with the tropical cyclone over Indian region in a coupled model.

Keywords. CFSv2; BMJ; cyclones; cumulus parameterization; convective precipitation.

1. Introduction

Accurate forecast of high impact weather events such as tropical cyclones (TC) remain a challenge to operational Numerical Weather Prediction (NWP) forecasters globally. Over the Indian region due to a long coast exposed to the Bay of Bengal and Arabian Sea and due to the vulnerability of the coastal population, the enhanced skill of TC forecast is the need of the hour. Some significant improvements have been accomplished in track error forecast of TC over the Indian seas (Deshpande *et al.* 2012; Mohapatra *et al.* 2013; Osuri *et al.* 2013; Kanase and Salvekar 2015a), but the intensity and heavy rainfall forecast still needs further improvement. Earlier studies (e.g., Saji and Ashrit 2014 and the references therein) have mostly used Weather Research and Forecasting

(WRF) Mesoscale model and its sensitivity to different physical parameterization (cumulus, PBL, microphysics, etc.) for evaluating model skill in TC forecasting. An important issue which pertains in forecasting cyclones is the model configuration. The mesoscale models and limited area models are widely used for dynamic forecasting of tropical cyclones. While these regional models can afford very high resolution over a domain of interest, it requires artificial lateral boundary conditions to be supplied externally which can limit its performance. Several studies have highlighted the issue for lateral boundary conditions and choice of domain in mesoscale simulations (Wu *et al.* 2005; Rauscher *et al.* 2006). In case of Bay of Bengal cyclones, there is a need to consider the dynamics over a wider domain. Since the TC genesis over the BOB occurs mainly because of either *in-situ* (which is associated with the disturbances as part of inter-tropical convergence zone) or from the low pressure systems which generally migrate from the east (Vitart *et al.* 2001). Impact of large scale environmental flow on the tropical cyclone intensity is well demonstrated by Krishnamurti *et al.* (1989). The effects of large scale circulations (larger than domain) can be incorporated in regional mesoscale models only through the lateral boundary conditions (Velden and Leslie 1991). Cyclone being a phenomenon of multi-scale interaction, for better forecasting of cyclones, it is very important to properly represent the large scale circulation and associated processes in the models. This can be achieved with the help of global models. Goswami *et al.* (2011) found that the variable resolution (VR) GCM and non-linear debiasing provide a skill score of ~ 0.5 in the forecasting of TC intensity 2–7 days in advance for 30 cases of TC over the Bay of Bengal. Tropical cyclone is a result of variety of physical processes at different scales interacting with the inner core dynamics and the large scale flow. Ocean being one of the important energy sources for a TC, there is a need of using ocean–atmosphere coupled models in the prediction of TC genesis and intensity changes. Hardly any attempts have been made in evaluating the skill of a coupled general circulation model (GCM) forecast for TC over the Indian seas for variety of cumulus physics. This is particularly needed as currently the GCM resolution is becoming finer than the mesoscale model and the GCM is being used for the TC forecast (Goswami *et al.* 2006, 2011). So there is a need to evaluate the coupled GCM performance with more physics to

identify better fidelity of the model for forecast application of TCs over the Indian seas.

Recent improvements in the dynamical ocean–atmosphere coupled numerical models are found to be useful for the simulation of weather phenomena involving multi-scale interaction. One of such dynamical model adopted under Monsoon Mission of Ministry of Earth Sciences, Government of India, is National Center for Environmental Prediction Climate Forecast System (NCEP CFS) which is fully coupled ocean–atmosphere–land model. NCEP CFS is extensively used for seasonal and extended range prediction (Yang *et al.* 2008; Abhilash *et al.* 2013; Sahai *et al.* 2014; Ramu *et al.* 2016; Rao *et al.* 2020) of the Indian Summer Monsoon and is under continuous development. Recently, the high resolution (T1534) atmospheric version of the CFSv2, i.e., GFS has been implemented for 10 days weather forecast over India (Mukhopadhyay *et al.* 2019).

Lim *et al.* (2014) had concluded that even though there is no change in the mean annual rainfall pattern due to increased spatial resolution, high resolution simulations are needed to capture short time-scale phenomenon as well as to reasonably represent the orographic precipitation. Goswami *et al.* (2015) explained the deficiencies in convective parameterization scheme of CFSv2 as one of the possible cause for dry precipitation bias over the Indian landmass. Recently, Abhik *et al.* (2017) showed that by improving the physical processes such as cloud microphysics, convection and radiation, the systematic bias of the model can improve significantly.

Accurate representation of cumulus processes in the model is one of the important factor which contributes to the model uncertainty and has large impact on the model rainfall prediction skills (Arakawa 2004; Krishnamurti 2005; Mukhopadhyay *et al.* 2010; Arakawa *et al.* 2011; Hong and Dudhia 2012; Pattanaik *et al.* 2013). For the purpose of proper representation of cumulus clouds, precise characterization of temperature and moisture fields in the sub-cloud layers and in the mid-troposphere is essential in the models (Yang *et al.* 1999). Palmer and Anderson (1994) found that large systematic errors of many models in simulating the monsoon rainfall are mainly due to convective parameterization. Similarly, Slingo *et al.* (1988) showed that the Asian summer monsoon and the onset dates are more sensitive to radiation and convective parameterization. Eitzen and Randall (1999) noted that increased

convective adjustment time in the model leads to the improvement in simulation of precipitation and upper level circulation in GCM. Thus, knowing the importance of cumulus processes, many weather and climate prediction centres have made significant efforts to develop and update their cumulus schemes for improving precipitation forecast skills (Tiedtke 1989; Han and Pan 2011). There are very limited studies of cumulus parameterization sensitivity using CFSv2 model particularly for the high impact weather phenomena like tropical cyclones. However, it will be worth mentioning that Vitart *et al.* (2001) made an interesting study using GFDL atmospheric GCM at T42 with 18 vertical levels and established that simulated tropical cyclone intensity and internal variability show significant sensitivity to the cumulus parameterization. Using the same dynamical core, they tested the sensitivity of a moist adjustment scheme of Manabe *et al.* (1965) and mass flux based scheme of Simplified Arakawa–Schubert (SAS) (Arakawa and Schubert 1974) and revised SAS. Contrary to this, Strachan *et al.* (2013) showed, using a hierarchy of atmospheric GCM with increasing resolution, that higher resolution better captures the tropical cyclogenesis. Both these papers addressed the important issue that for a realistic simulation of TCs, cumulus parameterization and model horizontal resolution both play a crucial role. However, these studies are conducted using an atmospheric GCM, but the impact of cumulus parameterization and horizontal resolution on TC intensity and its internal variability is not yet studied using ocean coupled GCM.

In all the earlier studies on the monsoon rainfall using CFSv2, simulations are done using default SAS available with CFSv2 model (Goswami *et al.* 2015; Abhik *et al.* 2016 and the references therein). Ganai *et al.* (2015, 2016) used RSAS in CFSv2 model and examined a 15-year climate free run. They found that RSAS is able to reduce some of the prominent biases related to diurnal rainfall, daily and seasonal mean rainfall as compared to SAS. Improvement is seen in the annual cycle, onset and withdrawal, but most importantly, the rainfall probability distribution function (PDF) has improved significantly. Ganai *et al.* (2019) further improved the limitations of RSAS by modifying the fractional cloud condensate to precipoitation conversion. Bombardi *et al.* (2015, 2016) studied impact of convective trigger mechanism on the tropical cyclone and monsoon simulations using CFSv2. They concluded that heated condensation

framework (HCF) as a convective trigger has improved the representation of convection vis-a-vis the monsoon rainfall and explained a way for improving the existing CP schemes by using different convection trigger mechanism. Ma and Tan (2009) have shown that slight modification in the connective trigger in CP scheme leads to large improvement in the sub-grid scale rainfall for TCs.

An attempt made by Mukhopadhyay *et al.* (2010) in simulating climatology of monsoon precipitation using WRF model, have shown that Betts–Miller–Janjic (BMJ) is able to simulate a reasonable heating profile, along with the realistic moist instability and seasonal cycle of evaporation and condensation and thus led to a better prediction of monsoon precipitation. Kanase *et al.* (2015) and Kanase and Salvekar (2015a, b), tried to understand the cloud and convective processes associated with the weak intensity storms formed over the Bay of Bengal. They found that, convective adjustment scheme such as Betts–Miller– Janjic (BMJ) is able to better reproduce the cyclone features than the mass flux based schemes. Slingo *et al.* (1996) showed improved simulation of UK Met Office model by the adjustment scheme as compared to mass flux scheme. Vaidya and Singh (2000) and Vaidya (2006) using limited area models showed that BMJ better simulates the rainfall and circulation features of monsoon depressions. Vaidya and Singh (1997) and Sun *et al.* (2015) also performed some sensitivity experiments with different adjustment parameters in BMJ and reported the impact of these parameters on different weather systems (depression, cyclones, etc.) particularly to improve the rainfall associated with these high impact weather systems.

There are some attempts (Bombardi *et al.* 2015, 2016) in modifying mass flux based convective schemes in CFSv2 which still could not resolve the model precipitation bias. The moist convective adjustment scheme, i.e., BMJ is able to produce the desirable forecast of the tropical cyclones in the regional mesoscale models. However, the convective adjustment scheme is not available in CFSv2 model. Here for the first time, we endeavour to implement a convective-adjustment scheme, i.e., BMJ in CFSv2 model. Fidelity of BMJ in CFSv2 model is tested and compared with the performance of SAS and RSAS schemes in CFSv2 for three Indian Ocean cyclones at three different resolutions, i.e., T126, T382 and T574.

The following questions are addressed in this study:

1. Do different cumulus parameterization schemes have an impact on cyclone intensity and its internal variability in coupled model?
2. Whether newly implemented moist convective adjustment scheme performs better for Indian Ocean cyclones especially the convective rainfall associated with the cyclones?
3. If yes, what could be the possible mechanisms behind the rainfall improvement?

Performance of BMJ cumulus scheme for cyclone simulation, more particularly the convective precipitation simulation, will allow us to further examine its fidelity in cyclone forecasting with a coupled model in Indian seas. Section 2 describes CFSv2 model along with experimental setup. Observed features of cyclones are mentioned in section 3. Results are discussed in section 4 followed by conclusion and future work in section 5.

2. Model description and experimental design

2.1 *Model description*

CFSv2 (Saha *et al.* 2014) used in the present study is a fully coupled ocean–atmosphere–land model. It consists of a spectral atmospheric model GFS (Global Forecast System) and Advanced version of the GFDL Modular Ocean Model, version 4p0d (MOM4). Ocean Model MOM4 (Griffies *et al.* 2004), is a finite difference model at 0.25–0.5° grid spacing with 40 vertical layers (10 m thickness from surface to 240 m, with 27 levels in the top 400 m to resolve the mixed layer). For the ocean model, resolution remains unchanged for all the experiments. For atmospheric model GFS, we considered three different resolutions, i.e., a spectral triangular truncation of 126 waves (T126, $\sim$110 km), 382 waves (T382, $\sim$35 km) and 574 waves (T574, $\sim$25 km) in the horizontal. Out of 64 levels in the vertical direction, there are 16 levels below 800 hPa and 27 levels above 150 hPa in the stratosphere (Saha *et al.* 2010). CFS model has rapid radiative transfer model (RRTM) for shortwave radiation with advance cloud radiation integration scheme (Iacono *et al.* 2000; Clough *et al.* 2005; Saha *et al.* 2014). Coupling of CFS is also done with four-layer Noah land-surface model (Ek *et al.* 2003) and a two-layer sea ice model (Wu *et al.* 1997; Winton 2000). Cloud microphysical processes are being represented by a simple formulation based on Zhao and Carr (1997). Detailed description of model can be found in Saha *et al.* (2006, 2010, 2014).

The two convection schemes are available in the atmospheric component of CFSv2 such as SAS convection (Hong and Pan 1998), and RSAS convection (Han and Pan 2011). In addition to SAS and RSAS, a convective-adjustment scheme, BMJ (Betts and Miller 1986; Janjic 1994, 2000) for cumulus parameterization is implemented in CFSv2. The details of the CFSv2 model description are available in several previous studies (e.g., Goswami *et al.* 2015; Abhik *et al.* 2016).

Here, we will highlight some of the major differences that exist between SAS and RSAS cumulus parameterization as this will be more relevant to the current study. Both SAS and RSAS follow a mass-flux approach to parameterize cumulus clouds. One fundamental difference between SAS and RSAS is the type of cloud model used in each scheme. An ensemble of clouds with different cloud tops exists in RSAS, whereas a single tall cloud type representation is used on SAS. The detrainment in SAS happens only at the top, whereas for RSAS, it can occur at various levels of the cloud (Han and Pan 2011). The BMJ scheme depends on cloud efficiency which again depends on the mean temperature of cloud, entropy change and precipitation (Betts and Miller 1986; Janjic 1994, 2000). The BMJ parameterization is a convective adjustment scheme, meaning that it determines 'reference' profiles of temperature and dew point towards which it nudges the model soundings at individual grid points. The first step in the scheme is to locate the most unstable (highest θ_e) model parcel within the lowest $\sim$200 mb above the ground. It lifts this parcel to its LCL (lifting condensation level), which it defines as cloud base. From there, the parcel is lifted moist adiabatically until the equilibrium level (EL) is reached. Cloud top is then defined as the highest model level at which the parcel is still buoyant, typically just below the EL. If the parcel is not buoyant at any level, convection is not activated and the scheme moves on to the next grid column. If the cloud is $<$ 200 mb deep, the scheme attempts to initiate shallow (non-precipitating) convection. Otherwise, it checks to see if deep (precipitating) convection can be activated. This scheme does not include the moist processes below the cloud base or in the lower boundary layer.

2.2 *Experimental design*

Three cases of North Indian Ocean cyclones formed over the Bay of Bengal in 2013 are selected for the study. Out of these three cyclones, two (Phailin and Lehar) were post-monsoon and one (Viyaru) was a pre-monsoon cyclone. The initial conditions for atmosphere and ocean are taken from NCEP Climate Forecast System Reanalysis (Saha *et al.* 2010). The model integration started from corresponding depression stage of each cyclone, i.e., for cyclone Phailin: 00Z08102018, for cyclone Lehar: 00Z23112013 and for cyclone Viyaru: 00Z10052018. For each cyclone case, total nine experiments are carried out with three cumulus parameterization schemes such as BMJ, SAS and RSAS scheme at T126, T382 and T574 model resolutions. Thus, total 27 experiments are performed. The model is integrated for 10 days including 24 hrs spin up in all the experiments. The output is saved at 6-hr intervals. The rest of the model configuration is same as discussed in model description. The observed features of cyclones are described in section 3.

3. Cyclone description

3.1 *Phailin*

Very Severe Cyclonic Storm (VSCS) Phailin was the most intense landfalling cyclone over the NIO after Odisha super cyclone of 29 October 1999, originated from a remnant cyclonic circulation from the South China Sea and termed as a depression over the Bay of Bengal on 0300 UTC of 08 October 2013. It further moved in north-westwards direction crossing Odisha and adjoining north Andhra Pradesh coast near Gopalpur (Odisha) around 1700 UTC of 12 October 2013. The observed minimum central sea level pressure (CSLP) and maximum, sustained surface wind (MSW) speed of Phailin are 940 hPa and 115 knots, respectively (RSMC Report 2014).

3.2 *Viyaru*

Cyclone Viyaru (10–16 May 2013) has the longest track over NIO in recent period after the VSCS Phet over Arabian Sea (June 2010). Its genesis took place near 5°N on 0900 UTC of 10 May 2013. It recurved north-eastward after an initial north-westward movement. It moved very fast on the day

of landfall (16 May 2013); such type of fast movement of cyclonic storm (CS) is very rare. Observed maximum, sustained surface wind speed (MSW) associated with the cyclone was ∼45 knots. The observed minimum central sea level pressure (CSLP) is 990 hPa (RSMC Report 2014).

3.3 *Lehar*

A depression formed over the south Andaman Sea on 23 November 2013, has intensified into a VSCS Lehar on 26 November (RSMC Report 2014). It has its first landfall near Port Blair around 0000 UTC 25 November as SCS (which is very rare and after November 1989 cyclone) and second landfall at Andhra Pradesh coast around 0830 UTC of 28 November as depression. The observed CSLP and MSW of Phailin are 980 hPa and 75 knots, respectively.

4. Results and discussion

4.1 *Surface parameters and vertical structure of cyclones at different resolutions*

The CFSv2 is run at three different resolutions for three cyclone cases of Phailin, Viyaru and Lehar. Figure 1 shows the track (a–c), track error in km (d–f), and intensity in hPa (g–i) and error in translational speed in ms^{-1} (j–l) of cyclone Phailin. The first column represents results with T126, second column shows results with T382 and results with T574 are presented in third column. Black line represents the best track of respective cyclones estimated by IMD, the blue line is for SAS, the green is for BMJ and track by RSAS is shown by red line. Broadly, the north-westward movement of the cyclone Phailin is captured by all the three cumulus schemes at all resolutions. Initially up to 72 hrs of model integration (figure 1), tracks by all the three CP schemes for all the three resolutions are almost overlapping. However, beyond 72 hrs of model integration, the track with RSAS shows large deviations from the best track as compared to BMJ and SAS. At T574 (∼27 km resolution), the observed track of the cyclone Phailin and model simulated track with BMJ and SAS are close to each other. The impact of CP and resolution is evident from the track error plots (figure 1d–f) for cyclone Phailin. Particularly with BMJ, the track error reduces with increase in resolution. The track error for BMJ and SAS is ∼150 km up to 144 hrs of
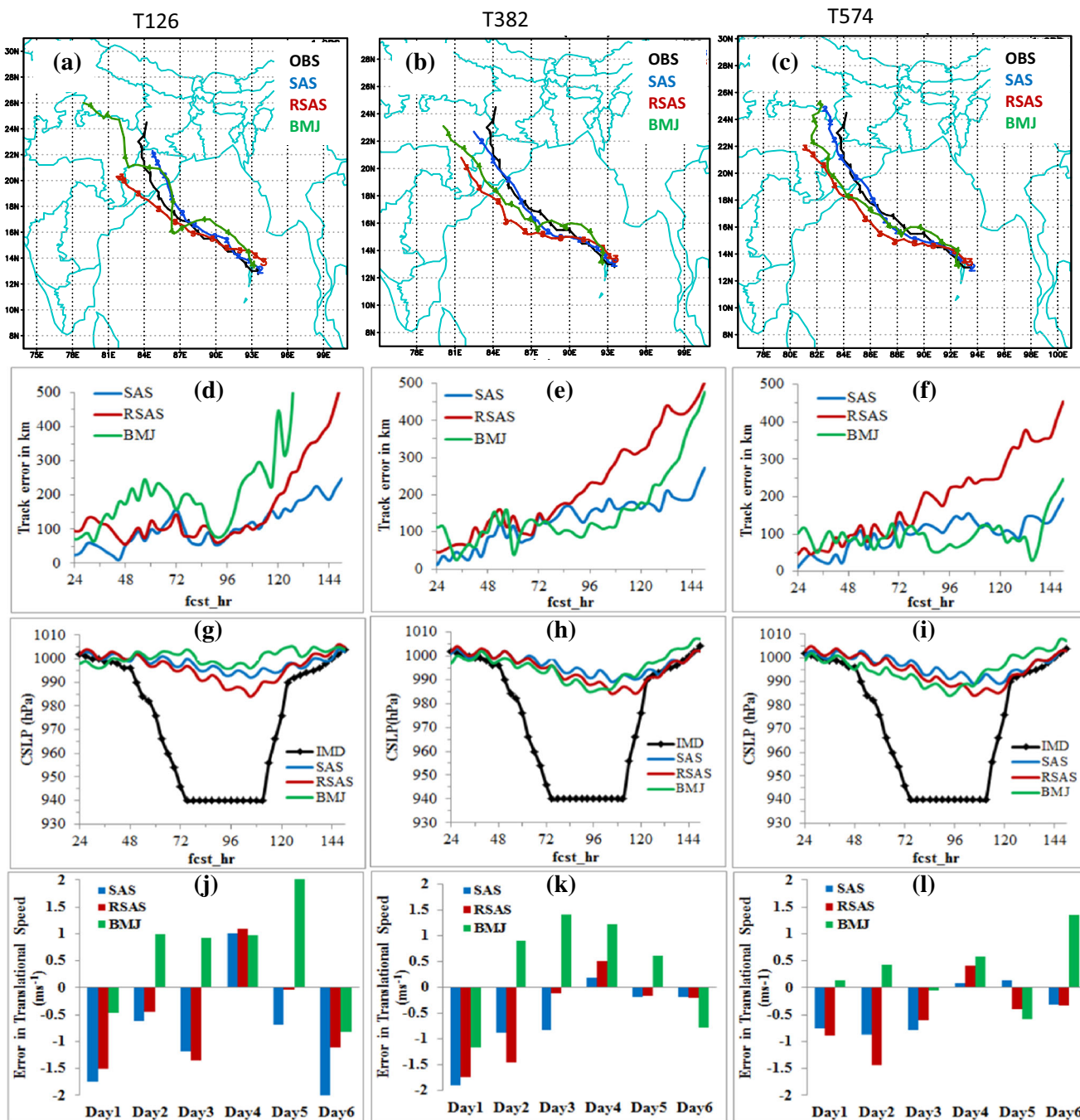
Figure 1. Observed and forecasted track (**a–c**), time evolution of track error in km (**d–f**), intensity in terms of CSLP (hPa) (**g–i**) and error in translational speed (ms^{-1}) of cyclone (**j–l**) all at three resolutions T126, T382 and T574, respectively, for cyclone Phailin. Colour indicates SAS (blue), RSAS (red), BMJ (green) and IMD (black).

model integration at T574. Strikingly, all CP schemes underestimate the intensity of the cyclone Phailin at all the resolutions. Inter-comparison between all the CP schemes (figure 1g–i) bring out that RSAS and BMJ simulate storm with marginally higher intensity than SAS at T382 ($\sim$38 km) and T574 ($\sim$27 km). In general, the intensity increases with resolution for all the CP schemes. Overall the performance of BMJ for predicting

track (track error is less for BMJ and SAS) as well as intensity (intensity is higher for BMJ and RSAS) is better than other CP schemes at higher resolution. Comparatively BMJ better predicts the track and intensity. The error in translational speed (figure 1j–l) is positive for BMJ for all lead times at all three resolutions. For SAS and RSAS, initially (for 2–3 days) the cyclone movement is very slow at all resolutions. But among all the CP

Table 1. *Different parameters (minimum CSLP (hPa), MSW (ms⁻¹), daily average track errors, landfall time) for cyclone Viyaru at three different resolutions.*

Cyclone Viyaru		CSLP (hPa)	MSW (ms^{-1})	Track error (km)			Landfall time
				Day 1	Day 2	Day3/Day4	
Obs.	IMD	990(117)	23	–	–	–	08UTC 16 May 2013
T126	BMJ	987(81)	58	110	182	254/552	12UTC 14 May 2013
	OSAS	992(105)	41	187	363	270/150	15UTC 14 May 2013
	RSAS	981(105)	68	135	167	124/297	15UTC 14 May 2013
T382	BMJ	986(69)	74	131	121	238/540	21UTC 13 May 2013
	OSAS	984(105)	80	142	216	62/134	12UTC 14 May 2013
	RSAS	986(105)	77	132	174	216/385	00UTC 15 May 2013
T574	BMJ	984(84)	79	142	199	244/437	00UTC 14 May 2013
	OSAS	982(93)	80	177	251	184/42	00UTC 15 May 2013
	RSAS	984(105)	76	145	165	228/371	00UTC 15 May 2013

The numbers in bracket show the hours of intensification from respective initial condition.

Table 2. *Same as table 1, but for cyclone Lehar.*

Cyclone Lehar		CSLP (hPa)	MSW (ms^{-1})	Track error (km)			Landfall time
				Day 1	Day 2	Day 3/Day 4	
Obs.	IMD	980(69)	39	–	–	–	0830UTC 28 Nov 2013
T126	BMJ	Could not simulate cyclonic circulation					
	OSAS	1002(69)	30	40	97	97/150	12UTC 26 Nov 2013
	RSAS	993(81)	54	30	50	51/96	12UTC 26 Nov 2013
T382	BMJ	995(81)	73	190	293	336/379	18UTC 27 Nov 2013
	OSAS	998(81)	56	36	58	104/92	09UTC 27 Nov 2013
	RSAS	998(93)	65	31	34	86/154	21UTC 26 Nov 2013
T574	BMJ	990(81)	46	190	301	353/463	12UTC 26 Nov 2013
	OSAS	1000(81)	42	90	143	120/230	12UTC 26 Nov 2013
	RSAS	995(81)	70	64	89	58/92	12UTC 26 Nov 2013

schemes, with increase in resolution, the error in translational speed is (less) close to observations for BMJ. Thus, with the track, intensity and translational speed, BMJ with T574 appears to be comparable with the observations. Track and intensity results are summarized in tables 1 and 2 for cyclones Viyaru and Leher. Thus increased resolution has more impact on the intensity simulation than on the track of the cyclone. Therefore, henceforth all the results will be discussed at T574. In the following section, further the basic features of the vertical thermodynamic structure of the cyclone are also discussed.

To understand the impact of CP schemes on the core structure of cyclone at the mature stage, the vertical cross section of various parameters are plotted in figure 2. The deviation of temperature with respect to layer average (figure 2a–c), vertical variation of horizontal wind speed in ms⁻¹ (figure 2d–f) at the corresponding mature stage of cyclone Phailin is plotted at T574 for three different CP schemes. Typical warm core structure with warming up to 9°C is observed in both RSAS and BMJ simulated cyclone, while SAS shows comparatively less warming ∼4°C (figure 2c). The simulated cyclone has extended up to 200 hPa level and it has its heating maxima at the mid-tropospheric levels. In BMJ and RSAS, the warm core extends down up to the ground. From figure 2(d–f), it is evident that strong winds with higher magnitude are well simulated by BMJ and RSAS as compared to SAS. The wind maxima also lie in the lower troposphere. Similar to Phailin, the vertical structure for the cyclones Viyaru and Lehar (figure not shown) also shows that higher intensity of the cyclones are associated with a strong warming in the middle troposphere associated with strong winds surrounding the center of the cyclone. In order to examine the impact of
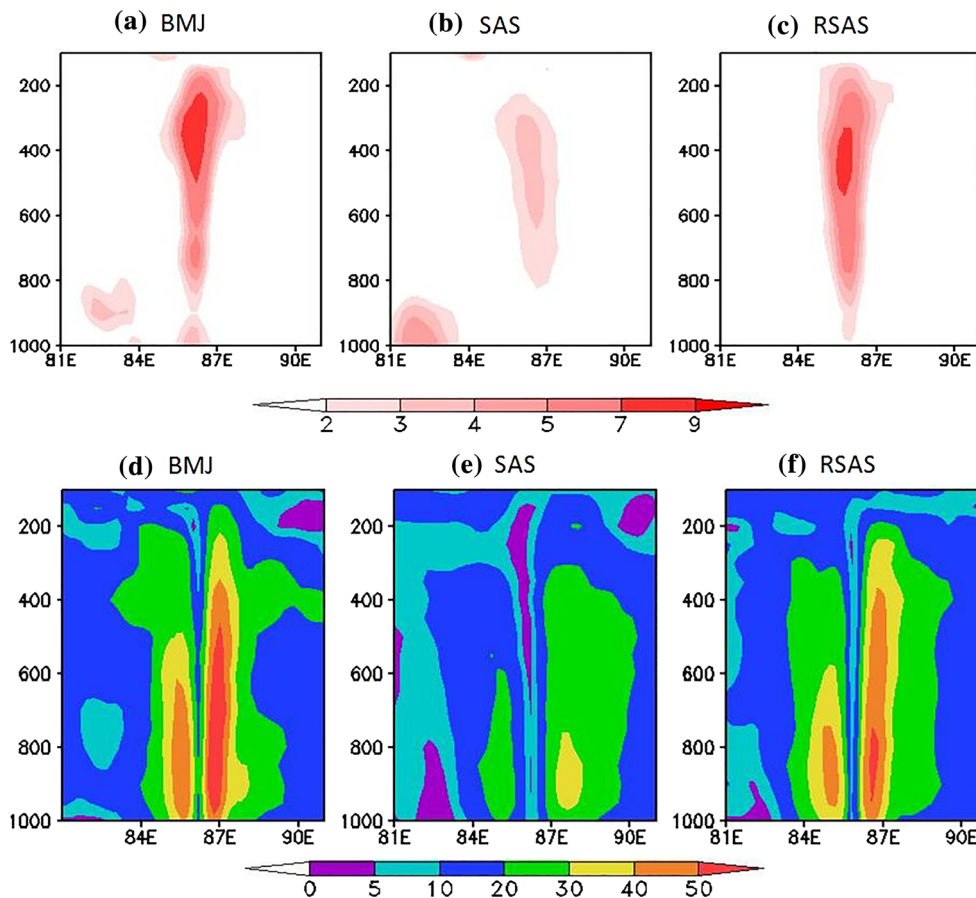
Figure 2. Deviation of temperature with respect to layer average in °C (**a–c**) and vertical variation of horizontal wind speed (ms^{-1}), (**d–f**) for BMJ, SAS and RSAS, respectively, at corresponding mature stage of cyclone Phailin. Mature stage for BMJ is at 21Z11Oct, SAS: 09Z12Oct, and RSAS: 09Z12Oct.

cyclone on ocean, difference between the sea surface temperature (SST) at the time of dissipation and formation are plotted for three CP schemes along with the real time global (RTG) SST observations (figure 3) for the cyclone Phailin. RTGSST data at 0.25 × 0.25° resolution, available at 3-hr interval are used in the present study. The negative values represent the cooling of the ocean surface and vice versa. Surface cooling of 2.1°C is seen in the observation. BMJ and SAS, reasonably indicate the cooling of ocean by about 2.5°C along the cyclone path, while RSAS underestimates the cooling.

Although the basic structure of cyclone is well simulated by all the CP schemes and is consistent with the intensity values simulated by CFSv2, our main objective is to study the simulation of intensity and the precipitation associated with the cyclones. Hence, we will now explore the reasons behind the different intensity behaviour for all the cyclones. The results for cyclone Phailin will be explained thoroughly.

4.2 *Rainfall*

Tropical rainfall measuring mission (TRMM) 3B42 V7 is used as observations in the present study. It is available at 0.25 × 0.25° resolution every 3 hrs. Details about the dataset can be found at http:// disc.gsfc.nasa.gov/precipitation/TRMM_README/ TRMM_3B42_readme.shtml (henceforth TRMM 3B42 v7 data is referred as observations in text). Daily accumulated total rainfall (mm) at 00Z10Oct, 00Z11Oct, 00Z12Oct and 00Z13Oct for each CP scheme along with observations is plotted for the cyclone Phailin (figure 4). Observations indicate intense (>180 mm day^{-1}) rain in the cyclone core region. For BMJ, the rainfall at the cyclone core region as well as in the rainbands is > 180 mm day^{-1} at most of the places, whereas it is underestimated by SAS and RSAS. The TC translational speed and intensity controls the rainfall distribution. Compared with other two schemes, BMJ better captures track, translational speed, intensity and rainfall distribution. To investigate
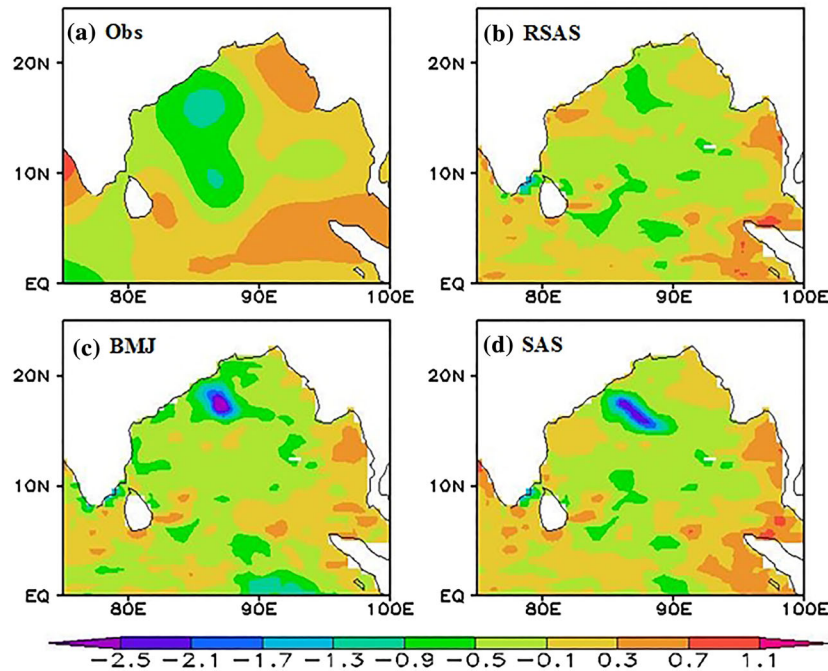
Figure 3. Difference between the sea surface temperature (SST) at the time of dissipation and formation of cyclone Phailin. (**a**) Obs, (**b**) RSAS, (**c**) BMJ, and (**d**) SAS.

further the contribution of the convective rain in the total precipitation, figure 5 shows the spatial pattern of convective rainfall for three CP schemes along with TRMM 3G68 as observations. TRMM 3G68 is an hourly gridded text (ascii) product containing 2A25 (Iguchi *et al.* 2000) rain estimates. It includes 24 hr of hourly grids into a single daily file. This information is further regridded uniformly on $0.25 \times 0.25°$ grid for fair comparison with the model. Observations indicate heavy convective rainfall (>150 mm day^{-1}) in the core of the cyclone. The rainfall intensity and distribution by BMJ better resembles with the observation considering the highest spatial correlation coefficient (top right corner of each panel). In SAS, the rainfall intensity is underestimated over a larger area, whereas RSAS produces a comparable amount of convective rain but largely overestimate the area of convective rain. The percentage contribution of convective rainfall to the total rainfall is plotted in figure 6 for all three convective parameterization schemes. BMJ simulates a realistic contribution of convective rain to total rain much similar to the observations. SAS and RSAS both significantly overestimate the contribution of convective rain to the total rain. The ratio of convective to non-convective rainfall averaged along the box (figure 6b) clearly indicates that SAS and RSAS overestimate the contribution of convective rain with respect to non-convective

rain. The ratio simulated by BMJ is comparable with the observations. To find out the physical mechanism responsible for the different behaviour of each CP scheme in simulating the convective rainfall, we have plotted the vertical profile of total cloud condensate (cloud water and cloud ice) averaged over $2 \times 2°$ around the cyclone center in figure 7. SAS and RSAS show lesser cloud condensate as compared to the BMJ in the lower as well as in the upper troposphere suggesting weaker convection associated with the cyclone core.

Underestimation of condensate by SAS and RSAS in the lower (higher) level may also affect the low (high) cloud distribution in the model compared to BMJ. It is well known from the literature (Mukhopadhyay *et al.* 2011; Kanase *et al.* 2015) that larger fraction of frozen condensate/ hydrometeors may lead to enhanced latent heat release and this may produce enhanced heating (Yanai *et al.* 1973) in the mid-troposphere (figure not shown here). The higher amount of cloud condensate produces large amount of mid-level heating and vice-versa in each CP scheme. The cloud water which is present at the lower levels is transported to mid-levels by strong vertical motions (figure not shown) in BMJ which further helps to build the deep clouds. In RSAS and SAS, relatively weak vertical motions result in the lesser amount of cloud water being transferred to
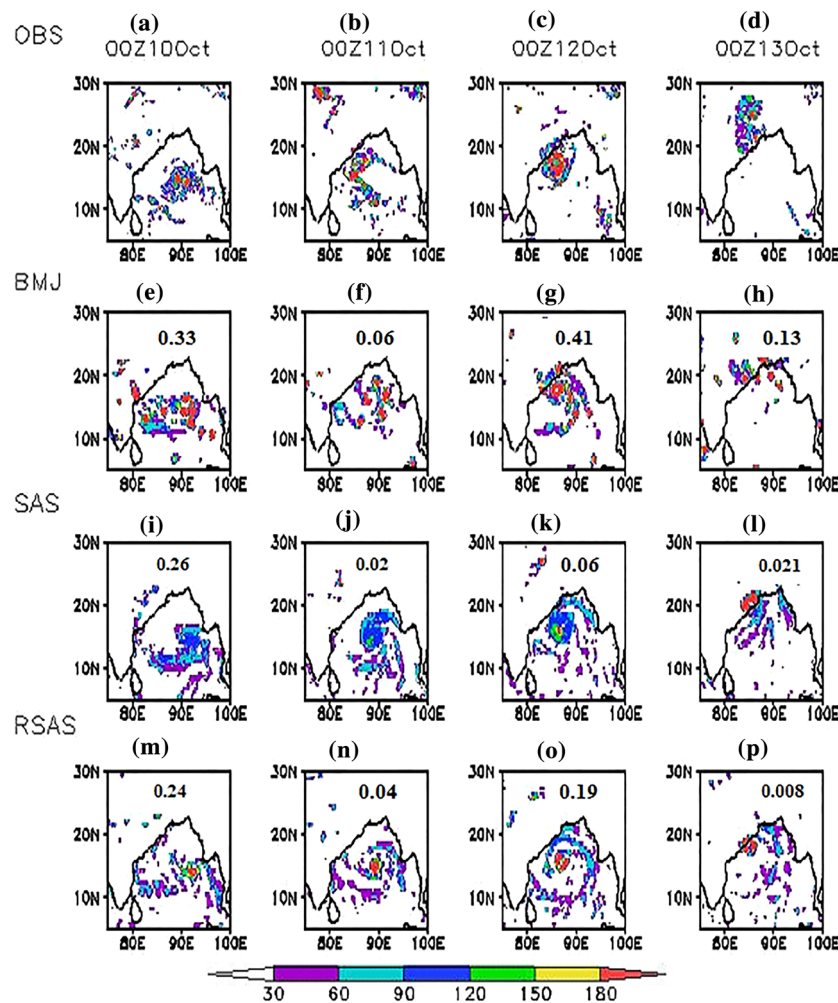
Figure 4. Total precipitation in mm/day for cyclone Phailin at 00Z10Oct, 00Z11Oct, 00Z12Oct, 00Z13Oct2013, respectively, in each column. Observations (**a–d**), BMJ (**e–h**), SAS (**i–l**) and RSAS (**m–p**), respectively. The number in each figure shows the spatial correlation coefficient (cc) between observations and model forecast.

mid-troposphere and within very short interval of time it is precipitated out resulting in more drizzling and lighter rain events. BMJ, on the other hand, produces deeper convection and due to increased vertical velocity, it helps the growth of deeper cloud and heavier rainrates around the cyclones.

Based on the analysis of figure 6, we hypothesize that SAS and RSAS possibly trigger the convection more frequently (Tirkey *et al.* 2019) than that in BMJ and eventually contribute more convective rain. To clarify more about the rainfall patterns, we have plotted daily accumulated cloud water path (figure 8a, d), precipitation (figure 8b, e) and precipitation efficiency (figure 8c, f) for total precipitation and convective precipitation. For this purpose, we have accumulated all the daily cloud water and daily precipitation (total as well as convective) for each cyclone, corresponding to a given precipitation bin (mm day^{-1}). The

precipitation bin of mm day^{-1} are based on the India Meteorological Department (IMD) classification of rainfall events. The precipitation efficiency f is defined as the ratio of precipitation rate to cloud water path. It has units of day^{-1} and it signifies that the higher values of f correspond to the shorter time scales for the conversion process (Li *et al.* 2012). For each bin, precipitation efficiency f is calculated by dividing the total daily precipitation amount by the corresponding total daily cloud condensate path. For cyclone Phailin (figure 8a, d), the total cloud condensate in BMJ is higher than in SAS and RSAS in all precipitation bins. For heavy precipitation bins of 115.5–204.4 mm day^{-1} and >204.4 mm day^{-1}, the cloud condensate in BMJ is one or two orders of magnitude higher than other two schemes. The precipitation amount resembles with the cloud condensate for all precipitation bins (figure 8b, d). For lighter
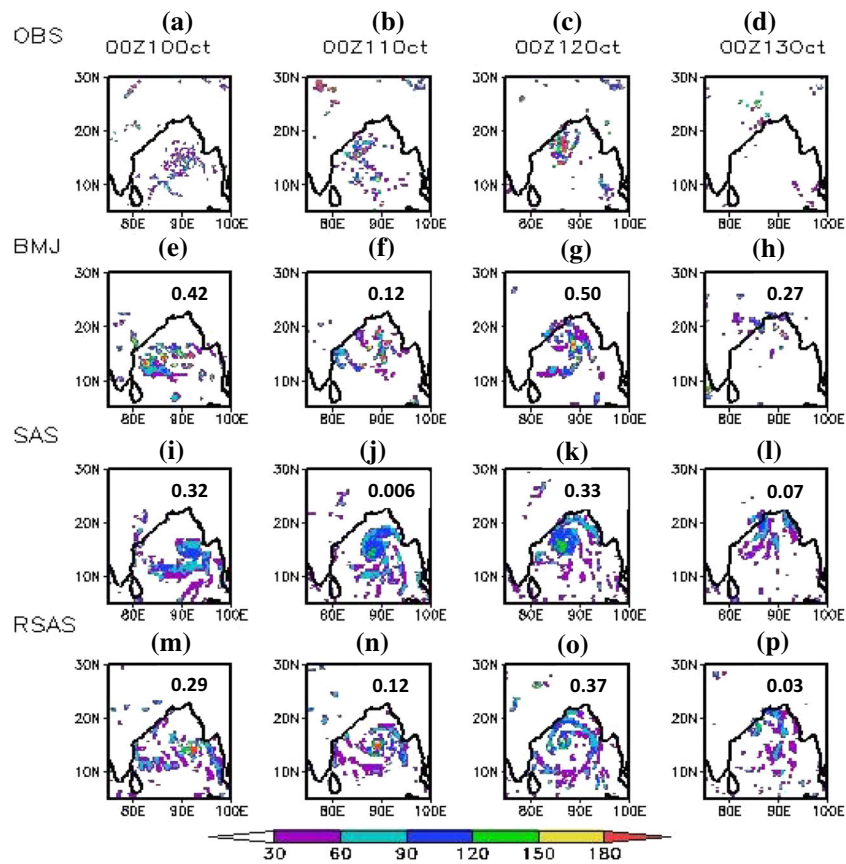
Figure 5. (**a–p**) Same as figure 4(**a–p**), but for convective precipitation (mm day^{-1}). The number in each figure shows the spatial correlation coefficient (cc) between observations and model forecast.
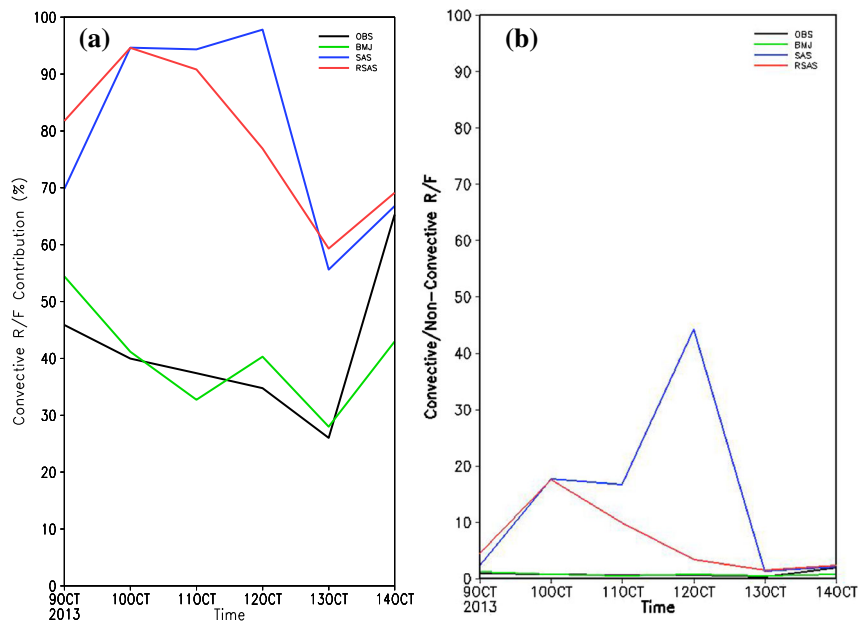

Figure 6. (**a**) Percentage contribution of convective rainfall to the total rainfall averaged over the area 81–96°E and 10–25°N (covers whole cyclone path). (**b**) Ratio of convective to non-convective rainfall averaged over the same box for cyclone Phailin. The black line represents observations for convective rainfall compared with the BMJ (green line), SAS (blue) and RSAS (red).
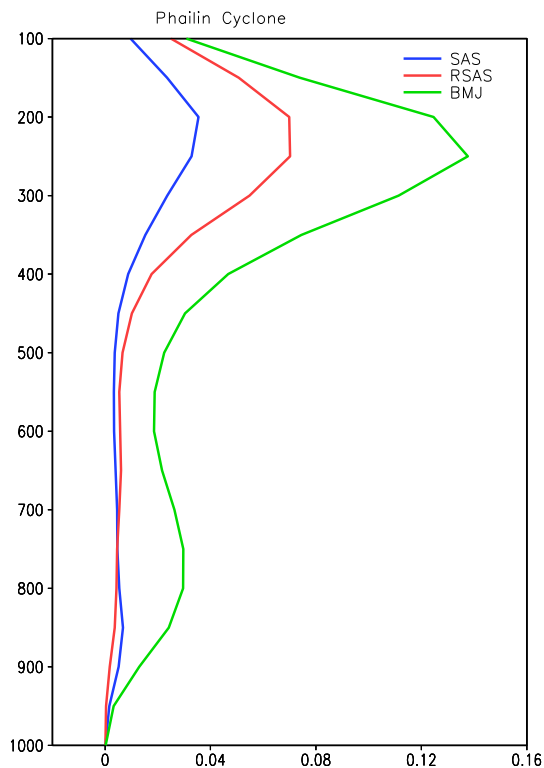
Figure 7. Total cloud condensate (including cloud water and cloud ice) in g kg^{-1} averaged over cyclone path for OSAS (blue), RSAS (red) and BMJ (green).

(bins below 64.5 mm rain) precipitation bin, the precipitation rate for all the three CP schemes is broadly similar but the differences in the magnitude of three CP scheme increase with heavy precipitation bins. Only BMJ gives the heavy precipitation which is also reflected in the precipitation efficiency. Lower values of f correspond to the larger time-scale for conversion of cloud water to precipitation and vice versa. Thus for BMJ, f shows lower values for all precipitation bins which correspond to the longer time required for conversion process when compared with RSAS and SAS. One remarkable point for BMJ, is more contribution of heavy rainfall bins (>115.5 mm day^{-1}) towards the total precipitation. In SAS and RSAS, precipitation is mostly dominated by light and medium rainfall events. The same conclusion can be drawn for cyclone Viyaru and Lehar (figures not shown). When we composite all the cyclones for the cloud water path, precipitation and precipitation efficiency, RSAS and SAS could able to convert the cloud condensate into precipitation in shorter time-scale which further add to the formation of drizzling precipitation events (figure not shown).

The above analyses indicate that BMJ is efficient in sustaining the convective instability and generating deep convection and heavier rain rates (>64 mm/day) than the SAS and RSAS. As such, SAS and RSAS trigger the convection more frequently and thus end up in generating more lighter and moderate rain rates. Zadra *et al.* (2014) studied the sensitivity of TC prediction skill to trigger adjustment in the convective parameterization. They found that the prediction skill improves with reduction in the activation frequency of convective scheme. In BMJ, it seems that there are deeper convection which led to the strengthening of TC intensity and generation of more intense precipitation. To investigate further, the number of grid points in each precipitation bins (as per IMD classification of rainfall events) are counted for convective rainfall (figure 9) during the cyclone period (from depression to dissipation stage). Here, an additional 'zero (0)' precipitation bin is added which means that the convective scheme is not triggered for these many grid points. The careful examination of number of grid points in zero precipitation bins clearly indicates that the BMJ scheme has triggered less often than RSAS and SAS in lower precipitation bins. The frequency distribution for convective precipitation (figure 9) shows that light precipitation events are larger in numbers for SAS and RSAS, whereas the heavy rainfall events are more for BMJ scheme. Overall, from the above discussion, it seems evident that BMJ scheme triggers convection less often than SAS and RSAS, thus adjusts the atmospheric profiles less frequently, leaving the atmosphere in a convectively unstable state. This allows the PBL to moisten and grow higher. Increased moisture in PBL injects more moisture from the lower troposphere to the mid-troposphere. The increase in the atmospheric moisture results in deep convective clouds, which in turn releases latent heat and feeds back to the large scale vis-à-vis increases the intensity and precipitation of the tropical cyclones. To further establish the relation between the instability and convective precipitation, scatter plot of convective precipitation and vertically integrated (between 950 and 100 hPa) moist static energy (MSE) is shown in figure 10. ERA5 analysis is used as the reference. It shows that, overall the moist instability pattern and magnitudes are realistically matching with BMJ. SAS underestimates the rain rates and the instability, while RSAS overestimates the rain rates but BMJ appears to produce a realistic MSE and rain rate relation.
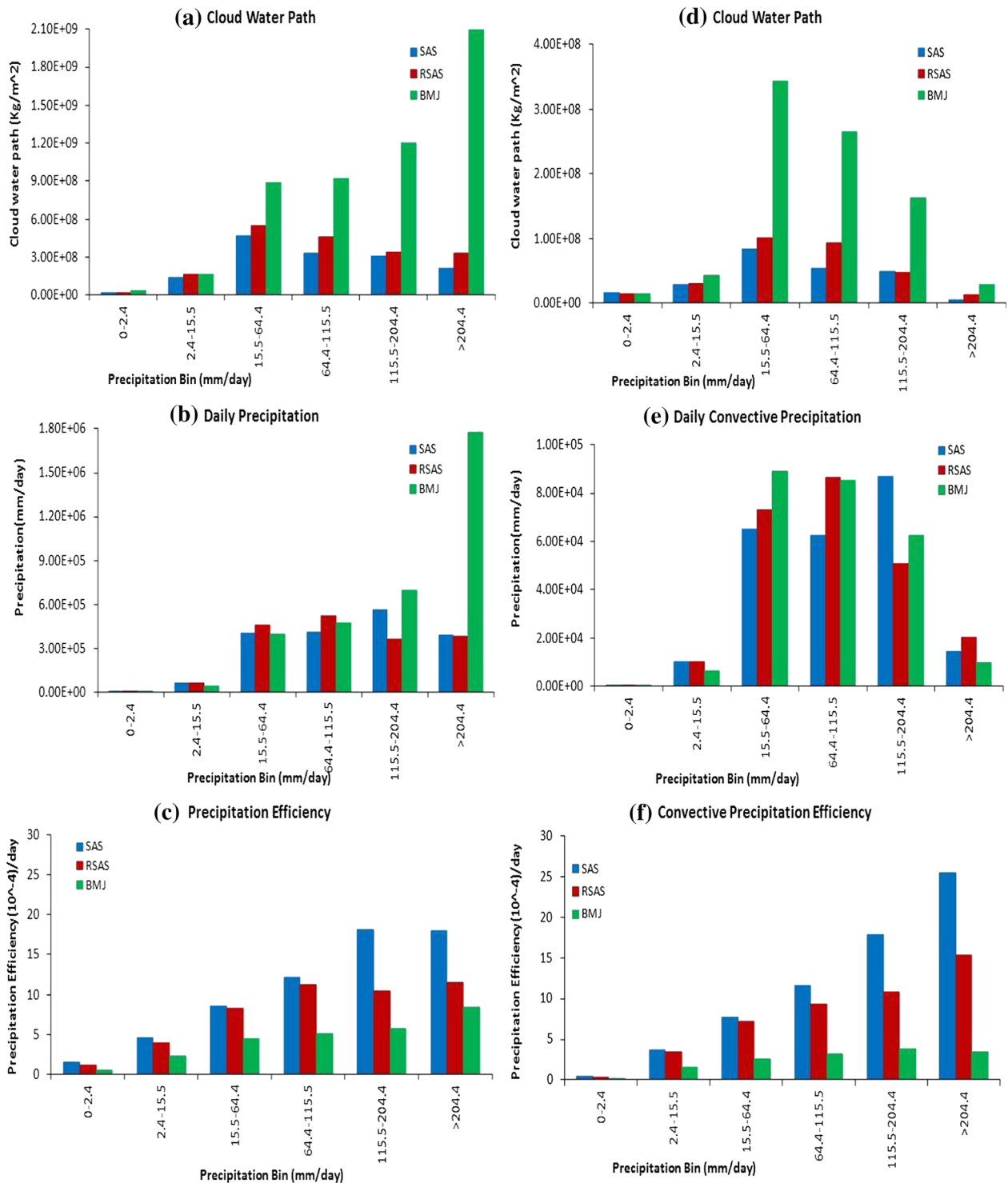
Figure 8. (**a**) Daily cloud water path (kg/m^2) for daily accumulated precipitation amount, (**b**) daily accumulated precipitation amount in each precipitation intensity bins of mm/day, (**c**) total precipitation efficiency (f) = Daily precipitation amount/Total cloud water path, (**d**) total cloud water path (kg/m^2) for daily accumulated convective precipitation amount, (**e**) daily accumulated convective precipitation amount in each precipitation intensity bins of mm/day, (**f**) convective precipitation efficiency (f) = Daily convective precipitation amount/Total cloud water path for convective precipitation.

The spatial plot of outgoing long wave radiation (OLR) from the Kalpana satellite observations (https://tropmet.res.in/~mahakur/Public_Data/ index.php?dir=K1OLR/3Hrly) are plotted with BMJ, SAS and RSAS (figure 11). OLR is 3 hourly data with 0.25 × 0.25° resolution. Details about
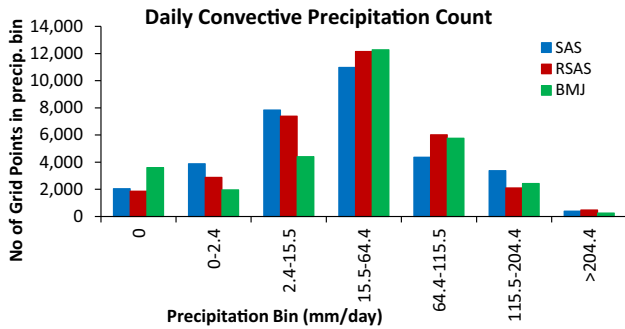
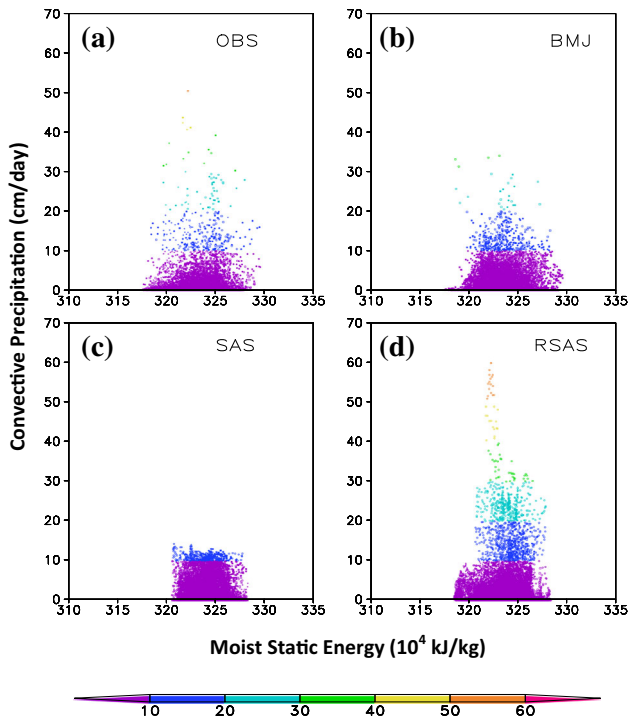Figure 9. Grid points count which lies in the respective convective precipitation bins.

Figure 10. Scatter plot of convective precipitation in (cm/day) and moist static energy (vertically integrated between 950 and 100 hPa) for (**a**) observations (ERA5 analysis), (**b**) BMJ, (**c**) SAS, and (**d**) RSAS. Colour bar indicates convective precipitation range.

the data can be found in Mahakur *et al.* (2013). It is evident that in the initial stages of the cyclone and at the time of landfall, BMJ captured the OLR reasonably well, though it has overestimated the convection in between. SAS produced a weaker OLR throughout the cyclone duration and RSAS simulated an overestimated OLR.

The joint probability density distribution (JPDD) (figure 12) is plotted to understand the association of precipitation and depth of cloud. Here OLR is considered as proxy for the depth of

the cloud. Lower OLR indicates deep clouds (Abhik *et al.* 2017). All rainfall events and OLR values are counted into 20 mm day^{-1} and 20 Wm^{-2} bins, respectively. The JPDD indicates the contribution of rainfall or OLR distribution which is expressed in percentage in a particular bin for the entire period. Lighter rain rates from the cloud with higher OLR (meaning lower level cloud) are evident in the observation and also reasonably captured by BMJ and SAS (figure 12). Probability distribution of moderate and heavier rain rate are also well captured by BMJ. SAS underestimates the deep cloud and overestimates the moderate and heavier rain rates. The RSAS also shows overestimation of moderate rain rates. Hence the most appropriate distribution of rain from the right type of clouds appears to be simulated by BMJ. Similar kind of conclusion can be drawn for Viyaru and Lehar cyclones (figures not shown).

5. Conclusions

In the present study, for the first time, we have implemented the Betts–Miller–Janjic (BMJ) cumulus parameterization scheme in NCEP Climate Forecast System version 2 (CFSv2) model and an attempt has been made to use the coupled (CFSv2) model to simulate three cyclones. Based on the previous promising results with BMJ parameterization scheme (Slingo *et al.* 1996; Mukhopadhyay *et al.* 2011; Kanase *et al.* 2015; Kanase and Salvekar 2015a, b), to improve the moist physical process especially the convective parameterization (CP) schemes in CFSv2, we have added one more CP scheme, i.e., BMJ in the model. Now BMJ, SAS and RSAS are the CP options available in CFSv2. To test this newly implemented CP scheme and evaluate its performance against SAS and RSAS and to evaluate the fidelity of coupled global model (CFSv2), three cases of tropical cyclones namely Phailin, Viyaru and Lehar of year 2013 are simulated.

The CFSv2 model is run with three different resolutions, i.e., T126 ($\sim$110 km), T382 ($\sim$38 km) and T574 ($\sim$27 km) with three CP schemes. Intercomparison between the track and intensity at three resolutions reveal that T574 better simulates the TCs than other two resolutions. It also shows that track is less sensitive to CP scheme, although CP schemes show significant sensitivity to cyclone intensity with BMJ producing highest intensity. In line with intensity, BMJ simulates a warm core and
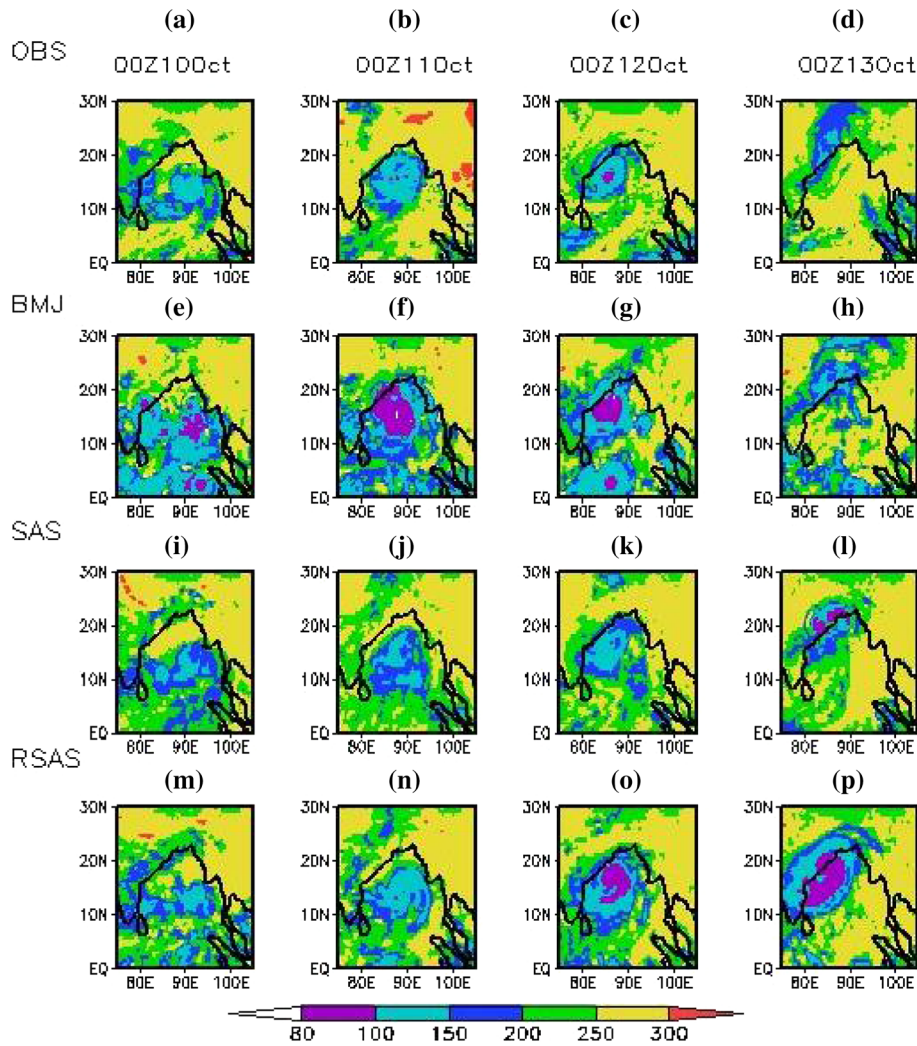
Figure 11. The outgoing long wave radiation (Wm^{-2}) in (**a–d**) observations, (**e–h**) BMJ, (**i–l**) SAS and (**m–p**) RSAS on 00Z10Oct, 00Z11Oct, 00Z12Oct, 00Z13Oct, respectively, in each column.

maximum wind comparable with the standard vertical structure of a cyclone. The 24 hrs accumulated rainfall when compared with the TRMM observations also shows that the rainfall in and around the cyclone centre is better represented in BMJ than SAS and RSAS. Further analyses showed that BMJ, among all the three CP schemes could able to produce a higher precipitation by converting cloud water to precipitation within relatively longer time, which helps in building and sustaining the deep convection, reducing lighter rain rate and eventually able to simulate a more intense storm. Other two CP schemes produce lighter precipitation with short interval of time in the conversion process. This result is consistent with Eitzen and Randall (1999).

Both SAS and RSAS overestimate convective rain, whereas BMJ scheme produces convective rain comparable with observation due to the fact that BMJ produces a deeper convection and does not trigger convection too often. BMJ appears to sustain the instability and deep convection longer and impact the cyclone intensity and heavy rainfall associated with it. It is also noted that BMJ is efficient in producing rain than SAS and RSAS. From the analyses of OLR and rain rate, BMJ appears to simulate a much realistic relation of cloud and precipitation. The moisture adjustment process in BMJ is efficient in sustaining the convective instability and generating deep convection and heavier rain than the SAS and RSAS. As such, SAS and RSAS trigger the convection more frequently thus end up in generating more lighter and moderate rain rates. In short, most appropriate distribution of rain from the right type of clouds are simulated by BMJ.

The paper argues that compared to available SAS and RSAS, BMJ scheme realistically produces
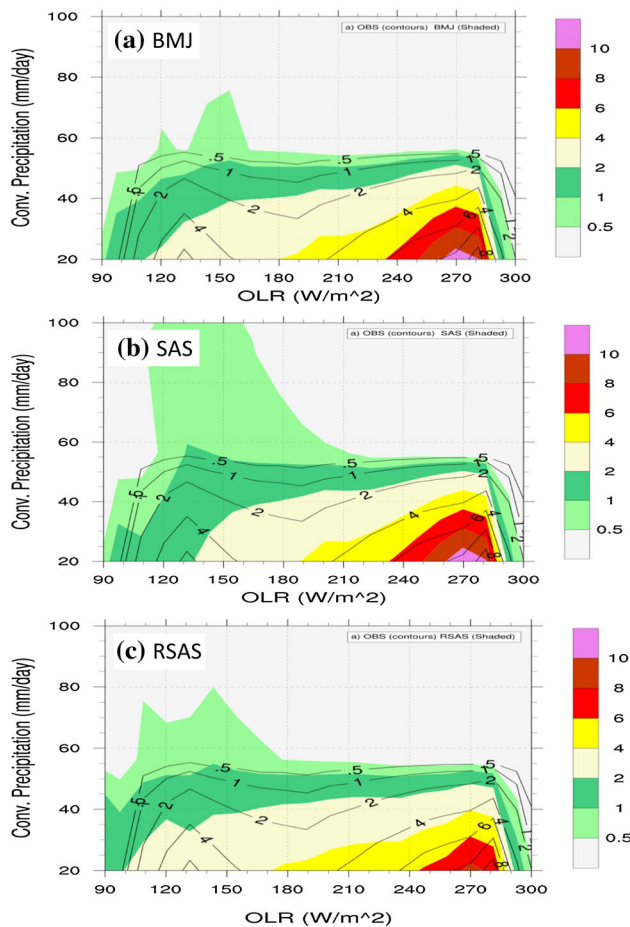
Figure 12. Joint probability density distribution of daily OLR (Wm^{-2}) and convective rainfall during cyclone period over the region 10–25°N, 82–97°E. The observed (OLR and TRMM rainfall) distribution is indicated in contours. The model distribution is shaded in each plot for CP scheme. (**a**) BMJ, (**b**) SAS, and (**c**) RSAS.

heavy precipitation associated with the tropical cyclone over the Indian region. This study also demonstrates that higher resolution coupled model could potentially be used for high impact weather events such as cyclones and thereby can provide a seamless forecasting framework from cyclone scale through extended to seasonal scale prediction based on CFSv2.

References

Abhik S, Mukhopadhyay P, Krishna R P M, Salunke K, Dhakate A R and Rao A S 2016 Diagnosis of boreal summer intraseasonal oscillation in high resolution NCEP climate forecast system; *Clim. Dyn.* **46** 3287–3303.

Abhik S, Krishna R P M, Mahakur M, Ganai M, Mukhopadhyay P and Dhudhia J 2017 Revised cloud processes to improve the mean and Intraseasonal variability of Indian summer monsoon in climate forecast system: Part 1; *J. Adv. Model Earth Syst.* **9** 1002–1029, https://doi.org/10.1002/2016ms000819.

Abhilash S, Sahai A K, Pattanaik S, Goswami B N and Arun K 2013 Extended range prediction of active-break spells of Indian summer monsoon rainfall using an ensemble prediction system in NCEP climate forecast system; *Int. J. Climatol.* **34** 98–113.

Arakawa A 2004 The cumulus parameterization problem: Past, present and future; *J. Climate* **17** 2493–2525.

Arakawa A and Schubert W H 1974 Interaction of a cumulus cloud ensemble with the large-scale environment. Part I; *J. Atmos. Sci.* **31** 674–701.

Arakawa A, Jung J-H and Wu C-M 2011 Towards unification of the multiscale modelling of the atmosphere; *Atmos. Chem. Phys.* **11** 3731–3742.

Betts A K and Miller M J 1986 A new convective adjustment scheme Part II: Single column tests using GATE wave, BOMEX, and arctic air mass data sets; *Quart. J. Roy. Meteorol. Soc.* **112** 693–709.

Bombardi R J, Tawfik A B, Manganello J V, Marx L, Shin C-S, Halder S, Schneider E K, Dirmeyer E K and Kinter III J L 2016 The heated condensation framework as a convective trigger in the NCEP Climate Forecast System version 2; *J. Adv. Model. Earth Syst.* **8** 1310–1329.

Bombardi R J, Schneider E K, Marx L, Halder S, Singh B, Tawfik A B, Dirmeyer P A and Kinter III J L 2015 Improvements in the representation of the Indian summer monsoon in the NCEP: The heated condensation framework as a convective trigger in the NCEP Climate Forecast System version 2; *Clim. Dyn.* **45** 2485–2498.

Clough S A, Shephard M W, Mlawer E J, Delamere J S, Iacono M J, Cady-Pereira K, Boukabara S and Brown P D 2005 Atmospheric radiative transfer modeling: A summary of the AER codes; *J. Quant. Spectrosc. Radiat. Transfer* **91** 233–244.

Deshpande M S, Pattanaik S and Salvekar P S 2012 Impact of cloud parameterization on the numerical simulation of a super cyclone; *Ann. Geophys.* **30** 775–795.

Ek M B, Mitchell K E, Lin Y, Rogers E, Grunmann P, Koren V, Gayno G and Tarplay J D 2003 Implementation of Noah land surface model advances in the National Centers for Environmental Prediction operational mesoscale Eta model; *J. Geophys. Res.* **108(D22)** 8851.

Eitzen Z A and Randall D A 1999 Sensitivity of the simulated Asian summer monsoon to parameterized physical processes; *J. Geophys. Res.* **104(D10)** 12,177–12,191.

Ganai M, Krishna R P M, Tirkey S, Mukhopadhyay P, Mahakur M and Han J-Y 2019 The impact of modified fractional cloud condensate to precipitation conversion parameter in revised simplified Arakawa–Schubert convection parameterization scheme on the simulation of Indian summer monsoon and its forecast application on an extreme rainfall event over Mumbai; *J. Geophys. Res.: Atmos.* **124**, https://doi.org/10.1029/2019JD030278.

Ganai M, Mukhopadhyay P, Krishna R P M and Mahakur M 2015 The impact of revised simplified Arakawa–Schubert convection parameterization scheme in CFSv2 on the simulation of the Indian summer monsoon; *Clim. Dyn.* **45** 881–902.

Ganai M, Mukhopadhyay P, Krishna R P M and Mahakur M 2016 The impact of revised simplified Arakawa–Schubert scheme on the simulation of mean and diurnal variability associated with the active and break phases of Indian summer monsoon using CFSv2; *J. Geophys. Res. Atmos.* **121** 9301–9323, https://doi.org/10.1002/2016jd025393.

Goswami B B, Deshpande M S, Mukhopadhyay P, Saha S K, Rao A S, Murthugudde R and Goswami B N 2015 Simulation of monsoon intraseasonal variability in NCEP CFSv2 and its role on systematic bias; *Clim. Dyn.* **28** 8988–9012.

Goswami P, Mandal A, Upadhyaya H and Hourdin F 2006 Advance forecasting of cyclone track over North Indian Ocean using a global circulation model; *Mausam* **57** 111–118.

Goswami P, Mallick S and Gouda K C 2011 Objective debiasing for improved forecasting of tropical cyclone intensity with a Global Circulation model; *Mon. Wea. Rev.* **139** 2471–2487.

Griffies S M, Harrison M J, Pacanowsk, R C and Rosati A 2004 A technical guide to MOM4; GFDL ocean group technical report 5 GFDL, 337p.

Han J and Pan H L 2011 Revision of convection and vertical diffusion schemes in the NCEP Global Forecast System; *Wea. Forecasting* **26** 520–533.

Hong D Y and Dudhia J 2012 Next-generation numerical weather prediction: Bridging parameterization, explicit clouds and large eddies; *Bull. Am. Meteorol. Soc.* **93** (Suppl.), https://doi.org/10.1175/2011bams3224.1.

Hong S Y and Pan H L 1998 Convective trigger function for a mass flux cumulus parameterization scheme; *Mon. Wea. Rev.* **126** 2599–2620.

Iacono M J, Mlawer E J, Clough S A and Morcrette J-J 2000 Impact of an improved longwave radiation model, RRTM, on the energy budget and thermodynamic properties of the NCAR Community Climate Model, CCM3; *J. Geophys. Res.* **105** 14873–14890.

Iguchi T, Kozu T, Meneghine R, Awaka J and Okamoto K 2000 Rain-profiling algorithm for the TRMM precipitation radar; *J. Appl. Meteor.* **39** 2038–2052.

Janjic Z I 1994 The step-mountain eta coordinate model: Further developments of the convection, viscous sublayer, and turbulence closure schemes; *Mon. Wea. Rev.* **122** 927–945.

Janjic Z I 2000 Comments on 'Development and evaluation of a convection scheme for use in climate models'; *J. Atmos. Sci.* **57** 3686.

Kanase R D and Salvekar P S 2015a Impact of physical parameterization schemes on track and intensity of severe cyclonic storms in Bay of Bengal; *Meteorol. Atmos. Phys.* **127** 537–559.

Kanase R D and Salvekar P S 2015b Effect of Physical parameterization schemes on track and intensity of cyclone LAILA using WRF model; *Asia-Pac. J. Atmos. Sci.* **51** 205–227.

Kanase R D, Mukhopadhyay P and Salvekar P S 2015 Understanding the role of cloud and convective processes in simulating the weaker tropical cyclones over Indian Seas; *Pure Appl. Geophys.* **172** 1751–1779.

Krishnamurti T N 2005 Weather and seasonal climate prediction of Asian summer monsoon, The Global Monsoon System: Research and Forecast; *WMO/TD No.* **1266** 342–375.

Krishnamurti T, Oosterhof D and Dignon N 1989 Hurricane prediction with a high resolution global model; *Mon. Wea. Rev.* **117** 631–669.

Li F, Rosa D, Collins W D and Wehner M F 2012 Super-parameterization: A better way to simulate regional extreme precipitation?; *J. Adv. Model Earth Syst.* **4** M04002, https://doi.org/10.1029/2011ms000106.

Lim S K-S, Hong S-Y, Yoon J-H and Han J 2014 Simulation of the summer monsoon rainfall over East Asia during the NCEP GFS cumulus parameterization at different horizontal resolutions; *Wea. Forecasting* **29** 1143–1154.

Ma L M and Tan Z M 2009 Improving the behavior of the cumulus parameterization for tropical cyclone prediction: Convection trigger; *Atmos. Res.* **92(2)** 190–211, https://doi.org/10.1016/j.atmosres.2008.09.022.

Mahakur M, Prabhu A, Sharma A K, Rao V R, Senroy S, Singh R and Goswami B N 2013 A high-resolution outgoing longwave radiation dataset from Kalpana-1 satellite during 2004–2012; *Curr. Sci.* **105(8)** 1124–1133.

Manabe S, Smagorinsky J and Strickler R F 1965 Simulated climatology of a general circulation Model with a hydrologic cycle; *Mon. Wea. Rev.* **93(12)** 769–798.

Mohapatra M, Nayak D P, Sharma R P and Bandyopadhyay B K 2013 Evaluation of official tropical cyclone track forecast over north Indian Ocean issued by India Meteorological Department; *J. Earth Syst. Sci.* **122(3)** 589–601.

Mukhopadhyay P, Taraphadar S, Goswami B N and Krishnakumar K 2010 Indian summer monsoon precipitation climatology in a high-resolution regional climate model: Impacts of convective parameterization on systematic biases; *Wea. Forecasting* **25** 360–387.

Mukhopadhyay P, Taraphdar S and Goswami B N 2011 Influence of moist processes on track and intensity forecast of cyclones over the north Indian Ocean; *J. Geophys. Res.* **116(D05116)** 1–21, https://doi.org/10.1029/2010JD014700.

Mukhopadhyay P *et al.* 2019 Performance of a very high-resolution global forecast syetm model (GFS T1534) at 125 km over the Indian region during the 2016–2017 monsoon seasons; *J. Earth Syst. Sci.* **128** 155, https://doi.org/10.1007/s12040-019-1186-6.

Osuri K K, Mohanty U C, Routray A, Mohapatra M and Nivogi D 2013 A real-time track prediction of tropical

cyclones over the north Indian Ocean using the ARW model; *J. Appl. Meteorol. Climatol.* **52** 2476–2492.

Palmer T N and Anderson D L T 1994 The prospects of seasonal forecasting – a review paper; *Quart. J. Roy. Meteor. Soc.* **120** 755–793.

Pattanaik S, Abhilash S, De S, Sahai A K, Phani R and Goswami B N 2013 Influence of convective parameterization on the systematic error of Climate Forecast System (CFS) model over the Indian monsoon region from an extended range forecast perspective; *Clim. Dyn.* **41** 341–365.

Ramu D A, Sabeerali C T, Chattopadhyay R, Nagarjuna R D, George G, Dhakate A R, Salunke K, Srivastava A and Suryachandra A R 2016 Indian summer monsoon rainfall simulation and prediction skill in the CFSv2 coupled model: Impact of atmospheric horizontal resolution; *J. Geophys. Res. Atmos.* **121** 2205–2221.

Rao Suryachandra A, Goswami B N, Sahai A K, Rajagopal E N, Mukhopadhyay P, Rajeevan M, Nayak S, Rathore L S, Shenoi S S C, Ramesh K J, Nanjundiah R, Ravichandran M, Mitra A K, Pai D S, Bhowmik S K R, Hazra A, Mahapatra S, Saha S K, Chaudhari H S, Joseph S, Pentakota S, Pokhrel S, Pillai P A, Chattopadhyay R, Deshpande M, Krishna R P M, Siddharth Renu, Prasad V S, Abhilash S, Panickal S, Krishnan R, Kumar S, Ramu D A, Reddy S S, Arora A, Goswami T, Rai A, Srivastava A, Pradhan M, Tirkey S, Ganai M, Mandal R, Dey A, Sarkar S, Malviya S, Dhakate A, Salunke K and Maini Parvinder 2020 Monsoon mission: A targeted activity to improve monsoon prediction across scales; *Bull. Am. Meteorol. Soc.* **100** 2509–2532, https://doi.org/10.1175/BAMS-D-17-0330.1.

Rauscher S A, Seth A, Qian J-H and Camargo S J 2006 Domain choice in an experimental nested modelling prediction system for South America; *Theor. Appl. Climatol.* **86** 229–246.

RSMC Report 2014 A report on cyclonic disturbances over North Indian Ocean during 2013; India Meteorological Department, New Delhi, India.

Saha S *et al.* 2006 The NCEP climate forecast system; *J. Clim.* **15** 3483–3517.

Saha S *et al.* 2010 The NCEP climate forecast system reanalysis. *Bull. Am. Meteorol. Soc.* **91** 1015–1057.

Saha S *et al.* 2014 The NCEP climate forecast system version 2; *J. Climate* **27** 2185–2208.

Sahai A K, Abhilash S, Chattopadhyay R, Borah N, Joseph S, Sharmila S and Rajeevan M 2014 High-resolution operational monsoon forecasts: An objective assessment; *Clim. Dyn.* **44** 3129–3140.

Saji M and Ashrit R 2014 Sensitivity of different convective parameterization schemes on tropical cyclone prediction using a mesoscale model; *Nat. Hazards* **73** 213–235, https://doi.org/10.1007/s11069-013-0824-6.

Slingo J M, Mohanty U C, Tiedtke M and Pearce R P 1988 Prediction of the 1979 summer monsoon onset with modified parameterization schemes; *Mon. Wea. Rev.* **116** 328–346.

Slingo J M *et al.* 1996 Intraseasonal oscillations in 15 atmospheric general circulation models: Results from an AMIP diagnostic subproject; *Clim. Dyn.* **12** 325–357.

Strachan J, Vidale P L, Hodges K, Roberts M and Demory M-E 2013 investigating global tropical cyclone activity with a hierarchy of AGCMs: The role of model resolution; *J. Clim.* **26** 133–152, https://doi.org/10.1175/jcli-d-12-00012.1.

Sun Y, Zhong Z, Dong H, Shi J and Hu Y 2015 Sensitivity of tropical cyclone track simulation over the western north pacific to different heating/drying rates in the Betts–Miller–Janjic scheme; *Mon. Wea. Rev.* **143** 3478–3494.

Tiedtke M 1989 A comprehensive mass flux scheme for cumulus parametrization in large-scale models; *Mon. Wea. Rev.* **117** 1799–1800.

Tirkey S, Mukhopadhyay P, Krishna R P M, Dhakate A and Salunke K 2019 Simulations of monsoon intraseasonal oscillation using climate forecast system Version 2: Insight for horizontal resolution and moist processes parameterization; *Atmosphere* **10** 429; https://doi.org/10.3390/atmos10080429.

Vaidya S S 2006 The performance of two convective parameterization schemes in a mesoscale model over the Indian region; *Meteorol. Atmos. Phys.* **92** 175–190.

Vaidya S S and Singh S S 1997 Thermodynamic adjustment parameters in the Betts–Miller scheme of convection; *Wea. Forecasting* **12** 819–825.

Vaidya S S and Singh S S 2000 Applying the Betts–Miller–Janjic scheme of convection in prediction of the Indian Monsoon; *Wea. Forecasting* **15** 349–356.

Velden C S and Leslie L M 1991 The basic relationship between tropical cyclone intensity and the depth of the environmental steering layer in the Australian region; *Wea. Forecasting* **6** 244–253.

Vitart F, Anderson J L, Sirutis J and Tuleya R E 2001 Sensitivity of tropical storms simulated by a general circulation model to changes in cumulus parameterization; *Quart. J. Roy. Meteor. Soc.* **127** 25–51.

Winton M 2000 A reformulated three-layer sea ice model; *J. Atmos. Ocean. Tech.* **17** 525–531.

Wu X, Simmonds I and Budd W F 1997 Modeling of Antarctic sea ice in a general circulation model; *J. Clim.* **10** 593–609.

Wu W, Lynch W A and Rivers A 2005 Estimating the uncertainty in a regional climate model related to initial and lateral boundary conditions; *J. Climate* **18** 917–933.

Yanai M, Esbensen S and Chu J-H 1973 Determination of bulk properties of tropical cloud clusters from large-scale heat and moisture budgets; *J. Atmos. Sci.* **30** 611–627.

Yang S, Zhang Z, Kousky V E, Higgins R W, Yoo S-H, Liang J and Fan Y 2008 Simulations and seasonal prediction of the Asian Summer monsoon in the NCEP climate forecast system; *J. Clim.* **21** 3755–3775.

Yang Y, Navon I M and Todling R 1999 Sensitivity to large-scale environmental fields of the relaxed Arakawa–schubert parameterization in the NASA GEOS-1 GCM; *Mon. Wea. Rev.* **127** 2359–2378.

Zadra A R, McTaggart-Cowan R, Vaillancourt P A, Roch M, Belair S and Leduc A M 2014 Evaluation of tropical cyclones in the Canadian global modelling system: Sensitivity of moist process parameterization; *Mon. Wea. Rev.* **142** 1197–1220.

Zhao Q and Carr F H 1997 A prognostic cloud scheme for operational NWP models; *Mon. Wea. Rev.* **125** 1931–1953.